0026-895X/87/040326-08$02.00/0

MOLECULAR PHARMACOLOGY, 31:326-333

Characterization of the Binding of a Morphine (μ) Receptor-Specific Ligand: Tyr-Pro-NMePhe-D-Pro-NH_2, [^{3}H]-PL17

STEVEN G. BLANCHARD, PAUL H. K. LEE, W. W. PUGH, J. S. HONG, and K.-J. CHANG

Department of Molecular Biology (S.G.B., K.-J.C.) and Medical Division (W.W.P.), Burroughs Wellcome Company, and National Institute of Environmental Health Sciences, Research Triangle Park, North Carolina (P.H.K.L., J.S.H.)

Received August 12, 1986; Accepted February 2, 1987

SUMMARY

The highly μ-receptor-selective ligand Tyr-Pro-NMePhe-D-Pro-NH_2 (PL17) was custom tritiated and its binding to rat brain membranes was directly measured. The data were well fit by a model assuming the existence of a single homogeneous population of binding sites. Scatchard analysis yielded values for K_d and binding sites of 6 nM and 0.16 pmol/mg, respectively. As expected for binding to an opiate receptor, addition of sodium, magnesium, and guanyl nucleotides to the assays resulted in a modulation of ligand binding. In all cases tested, however, no significant deviations of the Scatchard plots from linearity were observed. Furthermore, displacement of [^{3}H]-PL17 by all opioid ligands tested was monophasic, consistent with simple competitive inhibition at a single binding site. The IC_{50} values thus obtained showed good agreement with previously published values determined using less selective radiolabeled ligands. The regional distribution of [^{3}H]-PL17 binding to rat brain was examined by *in vitro* autoradiography. The labeling pattern was similar to that seen for other μ-type ligands. Because of its high selectivity, the binding of [^{3}H]-PL17 to the μ-type receptor can be measured directly without the need to suppress binding to other sites. As such, [^{3}H]-PL17 should be a useful ligand for dissecting the actions of multiple opiate receptors.

The existence of multiple opiate receptors was originally postulated by Martin and co-workers (1, 2) on the basis of the observed pharmacological effect of various opioids in the chronic spinal dog. Further evidence for multiple receptors came from studies of the potencies of various opioids in different isolated tissues. For instance, Lord *et al.* (3) reported a difference in the rank order of potency of opioid drugs in the mouse vas deferens versus the guinea pig ileum and postulated the existence of receptors of different selectivity in these tissues. Multiple opiate receptors have also been defined on the basis of their biochemical properties. Thus, the relative affinities of opioid ligands have been used as the basis to define a number of receptor types in rat brain. μ-Receptors bind morphine more tightly than do δ-receptors, while the relative affinities of the two receptor types are reversed for the enkephalins (4). Rat brain also contains ϵ-receptors which have high affinity for β-endorphin (5). Further evidence supporting the existence of these receptor types came from studies of their distinct autoradiographic distribution (6–9).

Although these studies have assumed that the receptor types are independent, some workers have proposed models involving interconversion (10) or allosteric interactions (11, 12) between the μ- and δ-receptors. Furthermore, the existence of subtypes of the μ-receptor has been postulated on the basis of a number of studies (13–16) using the quasi-irreversible antagonist naloxazone to block a specific population of high affinity receptor sites. Pasternak *et al.* (13) have termed these sites μ_1 and μ_2. The μ_1 site has high affinity for both enkephalins and morphine and is inactivated by naloxazone, whereas the μ_2 site corresponds to the more usual μ site, being selective for morphine over enkephalin (17).

As the models for multiple opiate receptors have become more complicated, so too have the experimental and data analysis methods. A number of computer-assisted curve-fitting and stimulation methods have been used to analyze the data in terms of the various proposed models (18–20). All of the multiple receptor classifications are based on the selectivity of a particular ligand for one receptor type over another. As such, the methods suffer from two major shortcomings. First, the selectivity of most ligands is not complete, so that contributions from other binding sites cannot be ignored. Second, in cases where there is high selectivity for a particular receptor type, the ligand has not been radiolabeled, so that its binding must be accessed by displacement of a relatively nonselective radioligand.

In the studies reported here, we have prepared [^{3}H]-PL17 (originally called PL017) and examined its binding to rat brain membranes. Like the parent compound, morphiceptin (21), PL17 has very high selectivity for μ-type receptors (22) so that contributions due to its binding to δ-type receptors can be

ABBREVIATIONS: PL17, Tyr-Pro-NMePhe-D-Pro-NH_2; DADLE, [D-Ala^2, D-Leu^5]enkephalin; DPDPE, cyclic [D-pennicilamine^2, D-pennicilamine^5] enkephalin; Gpp(NH)p, guanyl imidodiphosphate; HPLC, high performance liquid chromatography.

ignored. Therefore, the binding of [3H]-PL17 to rat brain membranes should reveal any subtype (μ_1 versus μ_2) interactions without the need for complex three (or more)-site analysis of the data.

Materials and Methods

Rat brain membranes. Brain membranes from male Sprague-Dawley rats (250–300 g) were prepared as previously described (4) and used fresh or stored at −90° until use. Control experiments showed that such storage did not alter the opiate binding properties of the membranes (data not shown).

Preparation and characterization of [3H]-PL17. [3H]-PL17 was prepared by catalytic tritiation of the dehydroproline precursor (New England Nuclear, Boston, MA). The purity of the labeled compound was determined by HPLC on a C_8 reverse phase column (150 mm, Absorbosphere) using a gradient of 0–50% acetonitrile in 0.1% trifluoroacetic acid. As shown in Fig. 1, a single peak of radioactivity comigrating with authentic PL17 was observed. Integration of the radioactivity recovered in this peak, however, could account for only ~85% of the applied material, suggesting the presence of low levels of radioactive impurities. Therefore, the [3H]-PL17 was purified using this HPLC system before further use.

Binding. Aliquots of brain membranes in 50 mM Tris, pH 7.7 (0.4–0.5 mg of protein, 0.5 ml total volume), were incubated with [3H]-PL17 and desired additions for 1 hr at room temperature unless otherwise noted. Nonspecific binding was determined in the presence of 10^{-6} M unlabeled PL17 or 10^{-6} M naloxone. No difference was observed in the background values determined with these two displacing ligands. All data are plotted after subtraction of the nonspecific values thus obtained. Nucleotide treatment of membranes was performed as previously described (23). Bound ligand was separated from free by collection of the membranes on Whatman GF/C glass fiber filters using an MACS 103 collector (Rocky Mountain Research Products, Boulder, CO) and the filters were washed twice with ice-cold buffer. Radioactivity retained by the filters was determined in an LKB 1212 liquid scintillation counter using Aquasol-2 as the scintillant. All points were determined in duplicate; errors were generally less than ±5% of the mean.

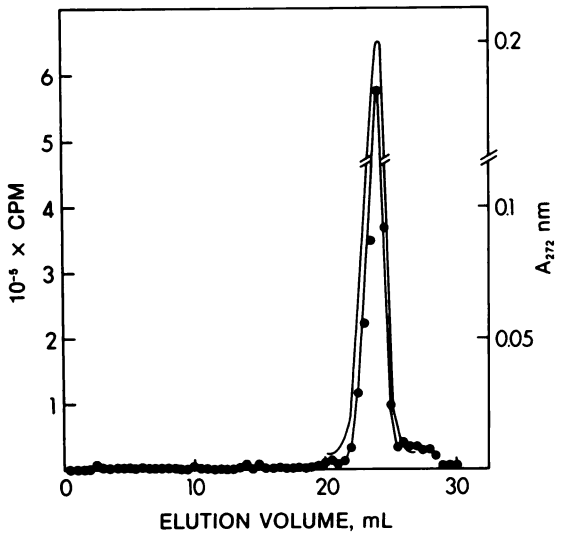

Fig. 1. Analysis of [3H]-PL17 by HPLC. A mixture of 2×10^{-7} unlabeled PL17 and ~2.7 μCi of [3H]-PL17 in 0.2 ml of water was injected onto a C_8 reverse phase HPLC column. Elution was with a 30-ml gradient of 0–50% acetonitrile in 0.1% trifluoroacetic acid. Fractions (0.5 ml) were collected and their radioactivity was determined (●). For purification, the unlabeled PL17 was omitted and the pooled radioactive peak fractions were lyophilized and then taken up in absolute ethanol. This purified stock solution was stored at −20°.

Autoradiographic localization of [3H]-PL17-binding sites in rat brain. The distribution of [3H]-PL17-binding sites in rat brain was assessed by *in vitro* autoradiography using standard techniques (6). Briefly, rats were sacrificed by decapitation and the brains were removed and rapidly frozen by immersion in isopentane cooled by a dry ice/methanol bath. Sections (10 μm) were cut on a cryomicrotome and thaw-mounted on gelatin-coated glass microscope slides. Sections were prefixed for 10 min at 0° in 170 mM Tris, pH 7.7, containing 0.5% formaldehyde followed by two 30-sec rinses in the same buffer without formaldehyde. Slides were incubated with [3H]-PL17 (3.3 nM) in the above buffer containing 5 mM magnesium for 1 hr at room temperature. Nonspecific binding was determined in the presence of 10^{-6} M unlabeled ligand. Free ligand was removed by sequentially dipping the slides for 5 sec into each of four beakers containing ice-cold buffer. After a final rinse in ice-cold distilled water the slides were dried with a stream of cold filtered air and exposed to Ultrafilm (LKB) for 3 months. Development was for 5 min in D-19 (Kodak) at 20° followed by a rinse in distilled water and fixation with Kodak fixer. Tissue sections were stained with 1% thionin for cytoarchitectural identification. Both the sections and the autoradiographic images were enlarged (Jena DL2) and drawn on tracing paper. These drawings were then overlayed and areas of increased [3H]-PL17 labeling were aligned with regional brain areas or specific nuclei according to the rat brain atlas of Paxinos and Watson (24).

Materials. [3H]-PL17 was custom tritiated by New England Nuclear. PL17, dehydroproline PL17, [Val4]morphiceptin, morphiceptin, and β-casomorphin were gifts of Dr. J. K. Chang (Pennisula Laboratories, San Carlos, CA). GTP and analogs were from Sigma (St. Louis, MO), and DPDPE was from Institute Armand-Frappier (Quebec, Canada). All other chemicals were of reagent grade or higher and were obtained from standard laboratory supply houses.

Results

Time and concentration dependence of [3H]-PL17 binding. As shown in Fig. 2, the association of specifically bound [3H]-PL17 with rat brain membranes was dependent on both the time of incubation and the amount of membrane protein added. At 24°, the half-time of binding was ~8 min at a ligand concentration of 7.3 nM (Fig. 2A). Maximum binding was reached in ~40 min; therefore, an incubation time of 1 hr was chosen for subsequent experiments to assure that equilibrium conditions had been reached. The half-time for dissociation of bound PL17 was determined to be 15 min (not shown). This was in excellent agreement with the value of 15.3 min calculated from the relationship $K_d = k_-/k_+$, where K_d is the equilibrium dissociation constant (4 nM, see Fig. 3B) and, k_- and k_+ (1.9×10^5 liters/mol/sec, Fig. 2A) are the dissociation and association rate constants, respectively. This slow half-time confirmed the validity of using a filtration method for separation of bound from free ligand since dissociation was slow with respect to filtration time. As shown in Fig. 2B, binding was linear up to 0.5 mg of membrane protein/tube. Higher concentrations tended to clog the glass fiber filters, resulting in high backgrounds and unreliable data. Therefore, the protein was fixed at 0.4–0.5 mg/tube for all experiments.

Determination of specific activity. In order to accurately determine the binding parameters for [3H]-PL17, it was necessary to know the specific activity of the labeled ligand. This could not be determined accurately, however, due to the limited amount of material that was prepared. Furthermore, purification of the ligand on HPLC may have changed the effective specific activity by removal of interfering impurities. Therefore, the specific activity was experimentally determined from competition curves of unlabeled PL17 against [3H]-PL17 as follows.

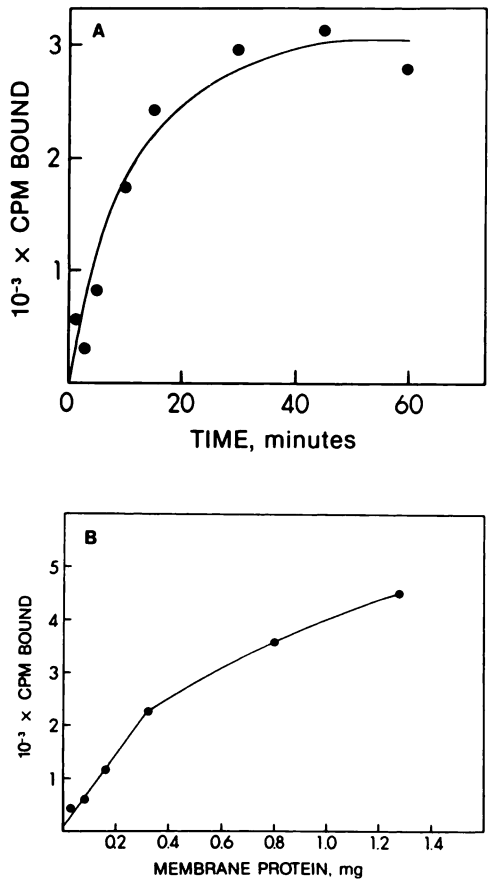

Fig. 2. Time and membrane concentration dependence of [^{3}H]-PL17 binding. A. Time course. The reaction was started by adding [^{3}H]-PL17 (final concentration 7.3 nM) to 10 ml of brain membranes (0.5 mg/ml in 50 mM Tris, pH 7.7) at 24°. At the indicated time points duplicate 0.5-ml aliquots were withdrawn and filtered through Whatman GF/C filters under vacuum. The filters were washed twice with 2-ml aliquots of ice-cold buffer, and the radioactivity remaining bound to the filters was determined. Nonspecific binding determined in a duplicate experiment containing 10^{-6} M unlabeled PL17 has been subtracted. The *points* are the average of duplicate determinations and the *solid line* represents the best fit to the equation $C_t = C\infty(1 - \exp(-kt))$ where C_t and $C\infty$ are the cpm bound at times t and equilibrium, respectively. Nonlinear least squares gave value of $C\infty$ = 3200 cpm and the value $k = 1.3 \times 10^{-3}$ sec^{-1}. This value for k corresponds to a second order rate constant of 1.9×10^5 liters/mol/sec. B. Membrane dependence. Various amounts of membrane protein were incubated with 5.2 nM [^{3}H]-PL17 for 1 hr at room temperature followed by filtration and determination of radioactivity as in A. *Points* are means of duplicate determinations. Nonspecific binding has been subtracted.

For simple competitive inhibition the inhibition constant, K_I, for a ligand is given by Eq. 1 (25).

$$K_I = IC_{50} \cdot (1 + L^*/K_d)^{-1} \quad (1)$$

where IC_{50} is the midpoint of the displacement curve, L^* is the concentration of radiolabeled ligand, and K_d is its dissociation constant. For the case where the labeled and unlabeled (displacing) ligands have the same affinity, $K_d = K_I = K$ and Eq. 1 simplifies to

$$IC_{50} = K(1 + L^*/K) \quad (2)$$

The concentration of radiolabeled ligand L^* is related to C^*, the amount of radioactivity added (in cpm), by the relationship $L^* = AC^*$ where A is the specific activity in terms of nM/cpm. Therefore, Eq. 2 can be written as

$$IC_{50} = K + AC^* \quad (3)$$

and a plot of IC_{50} determined at various concentrations of radioactive ligand will be linear with an intercept of K and a slope equal to the specific activity. Fig. 3B illustrates such a plot with least squares fit parameters of K = 3.96 nM and $A = 3.66 \times 10^{-5}$ nM/cpm. Since the assay volume was 0.5 ml, this corresponds to 1.83×10^{-8} nmol/cpm. This calibration value was used for all calculations. Because the specific activity is determined directly under the particular experimental conditions employed, the difficulties involved in determining counting efficiencies are avoided. Eq. 3 is valid where the radiolabel does not chemically perturb the ligand (e.g., tritium) but may not hold true for labels such as iodine where the label may modify the chemical properties of the ligand. In such cases the validity of the assumption that the labeled and unlabeled

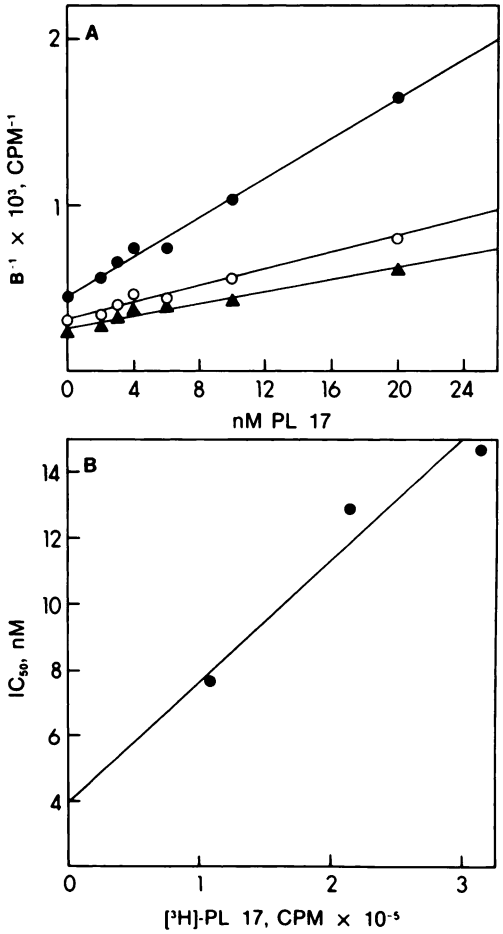

Fig. 3. Calibration of [^{3}H]-PL17 specific activity. A. Displacement curves of cold PL17 (2–20 nM) versus [^{3}H]-PL17 are shown plotted in the form $\frac{1}{B} = \frac{1}{B_0} + \frac{1}{B_0 IC_{50}} \cdot L$(Dixon plot), where B and B_0 are the values for bound ligand at ligand concentrations L and at zero ligand, respectively. The corresponding IC_{50} values calculated from the least squares values of the slope and intercept (correlation coefficients were ≥0.98) and total [^{3}H]-PL17 used were: 7.67 ± 0.11 nM, 1.08×10^5 cpm/0.5 ml (●); 12.9 ± 0.1 nM, 2.14×10^5 cpm/0.5 ml (○); 14.7 ± 0.2 nM, 3.15×10^5 cpm/0.5 ml (▲). B. Plot of the data from A according to Eq. 3. Linear least squares gave K = 3.96 nM and $A = 3.66 \times 10^{-5}$ nM/cpm (correlation coefficient = 0.967).

ligands have similar receptor binding properties must be experimentally determined (26).

Saturation binding of [^{3}H]-PL17. As shown in Fig. 3A, plots of 1/bound versus PL17 added did not deviate significantly from a straight line, suggesting that the competition of PL17 with [^{3}H]-PL17 was at a single site. To further confirm this, saturation binding of [^{3}H]-PL17 to brain membranes was carried out. The resulting data are presented in Fig. 4 as a Scatchard plot (27). Although some scatter in the experimental data was evident, no deviation from linearity was observed and the data were well fit by linear least squares with a slope of -0.166 nM^{-1} and an intercept of 0.027 (correlation coefficient -0.923) corresponding to an apparent K_d of 6 nM and a concentration of binding sites of 0.16 nM. Note that this value for K_d was in good agreement with the value of 4 nM obtained by extrapolation of the calibration plot in Fig. 3B to zero [^{3}H]-PL17 concentration.

Effects of guanyl nucleotides and cations. Both sodium ions (100 mM) and the nonhydrolyzable guanine nucleotide analog Gpp(NH)p (10^{-4} M) decreased binding of [^{3}H]-PL17. As shown in Fig. 4, this decrease could be explained by a decrease in both the number of binding sites and the affinity of [^{3}H]-PL17. Although some nonlinearity is apparent in the presence of Gpp(NH)p, the very low binding in this case (<100 cpm for the points which apparently deviate from linearity) makes unambiguous determination of the presence of high affinity binding sites difficult. When both compounds were included in the assay, binding was reduced to essentially zero (data not shown). In contrast, magnesium ion had little effect on either the affinity or the number of binding sites (Fig. 4). As previously demonstrated for ^{3}H-DADLE at both μ and δ sites (23), however, pretreatment of membranes with 10^{-4} M GDP followed by washing and assay of [^{3}H]-PL17 binding in the presence of magnesium resulted in an increase in the number of binding sites to 173% of the untreated control, whereas the apparent K_d values for treated and control were 7.2 and 6 nM, respectively.

Displacement of [^{3}H]-PL17 binding by opioid ligands. In order to further characterize the binding properties of [^{3}H]-PL17, the ability of a number of other opioid drugs to displace bound [^{3}H]-PL17 was examined. As shown in Fig. 5, the displacement curves for the tested μ-selective drugs could all be fit to a simple competitive model assuming only one binding site; no clear evidence for a more complicated displacement was observed. Furthermore, the IC_{50} values observed were in excellent agreement with those previously determined using less selective μ-radiolabels (Table 1) (21, 22). Note that [Val^4] morphiceptin corresponding to the morphiceptin peptide contained in the sequence of human β-casein had a high potency, whereas the δ-receptor-selective peptide DPDPE had low potency in competition with [^{3}H]-PL17 binding.

Autoradiographic localization of [^{3}H]-PL17 binding in rat brain. The distribution of μ-receptors, as revealed by labeling of rat brain slices with [^{3}H]-PL17, was very similar to that reported previously (7). A typical clustering distribution was observed in caudate (Fig. 6). A particular advantage of

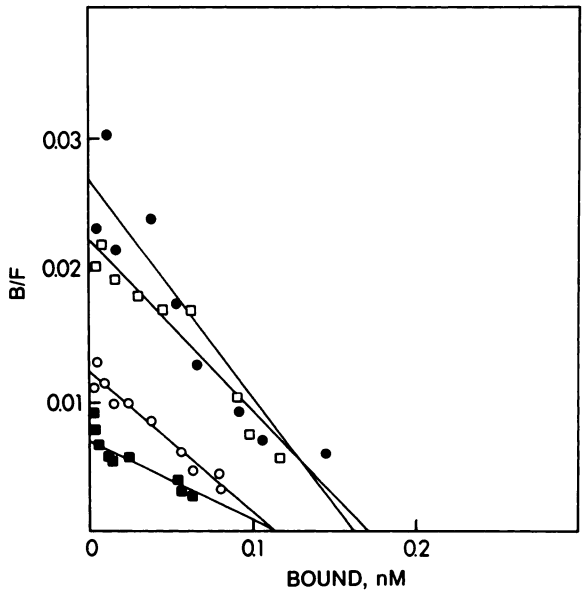

Fig. 4. Scatchard plots of [^{3}H]-PL17 binding to rat brain membranes. Data show binding in the presence of: no additions, K_d = 6 nM, R_0 = 0.16 nM (●); 0.1 M NaCl, K_d = 9.3 nM, R_0 = 0.12 nM (○); 10^{-4} M Gpp(NH)p, K_d = 17.1, R_0 = 0.12 (■); 25 mM $MgCl_2$, K_d = 7.6 nM, R_0 = 0.17 nM (□). Values of K_d and R_0 were calculated from the slope and intercept estimated by linear least squares of the data; correlation coefficients were ≥0.9 in all cases. All points were determined in duplicate and a single membrane preparation was used to allow direct comparisons of the individual treatments.

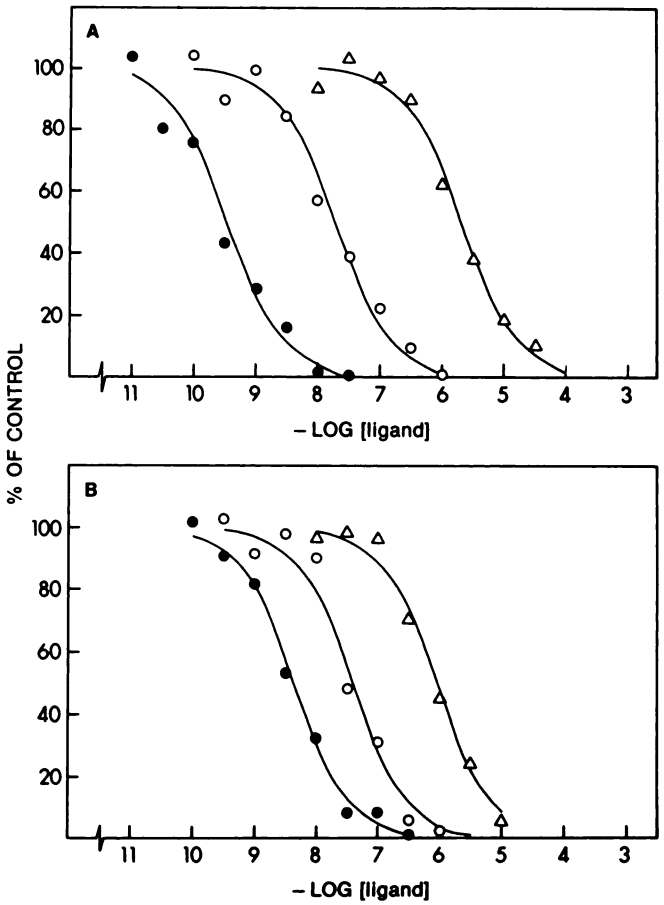

Fig. 5. Displacement of [^{3}H]-PL17 by various unlabeled ligands. The *solid lines* are theoretical fits to a simple binding isotherm using IC_{50} values calculated from the data points as described in the legend to Fig. 3A. A: △, β-casomorphin, IC_{50} = 2130 nM; ○, [Val^4]-morphiceptin, IC_{50} = 36 nM; ●, morphine, IC_{50} = 0.3 nM. B: △, DPDPE, IC_{50} = 490 nM; ○, morphiceptin, IC_{50} = 60 nM; and ●, DADLE, IC_{50} = 4.8 nM. The data shown are for a single representative experiment. Average values from three separate determinations are listed in Table 1.

TABLE 1

IC_{50} values for displacement of [^{3}H]-PL17 by opioid ligands

Ligand	K_i[a]	IC_{50}[b]
	nM	nM
Morphine	0.3 ± 0.02 (3)	0.4
DAGO[c]	1.9 ± 0.2 (3)	
DADLE	4.9 ± 1.3 (3)	4
[Val^4]Morphiceptin	16.1 ± 1.0 (3)	37
Morphiceptin	34.9 ± 6.4 (3)	63
DPDPE	490 ± 90 (3)	
β-Casomorphin	1160 ± 300 (3)	6500

[a] Determined by inhibition of [^{3}H]-PL17 binding. Values are expressed as averages ± standard deviations. Numbers in parentheses denote the number of times each experiment was repeated.

[b] Determined by inhibition of ^{125}I-FK 33,824 (0.3 nM), except for β-casomorphin which was determined against [^{3}H]naloxone. Data are from Refs. 22 and 35.

[c] DAGO, [D-Ala^2, NMePhe^4·Gly^5-ol]enkephalin.

[^{3}H]-PL17 as a ligand for autoradiographic localization of μ-receptors was its low background. Under the conditions used in Figs. 6–8, no detectable nonspecific labeling was observed. The most heavily [^{3}H]-PL17-labeled structures in the two sections presented in Figs. 7 and 8 were accumbens nucleus, stria medullaris, medial thalamus, hypothalamus, amygdala, inferior colliculus, and interpeduncular nucleus. In Fig. 7, a coronal section located approximately 3.5 mm posterior to bregma, light labeling in cortex is restricted to a band in layer V of frontal and parietal cortices. Also, light labeling is seen in the CA2 region of the hippocampus. Moderate to heavy labeling is spread throughout medial and interlaminar thalmic nuclei, and extends ventrally to include medial hypothalamus. In the amygdala, the heaviest labeling is seen in basolateral, basomedial, and central amygdaloid nuclei. Also notice the strong bands of labeling located in the stria terminalis and fundus striati on the right side of the section.

A sagittal section located approximately 0.5 mm lateral to the midline is presented in Fig. 8. Heavy labeling is seen in nucleus accumbens intersperced with the islands of Cájàl. Two very densely labeling spots, the stria medullaris, are present in the habenula nucleus. In the thalamus, moderate labeling can be seen in the paraventricular, central medial, and reticulotegmental nuclei. Very heavy labeling is present caudally, in the ventrally located interpeduncular nucleus, while strong labeling can be seen in the dorsally situated inferior colliculus. Also note a light band of labeling in the superficial grey layer of the superior colliculus.

Discussion

An important feature of the present study is that the specific activity of the radiolabeled PL17 was determined experimentally on the basis of its ability to displace unlabeled PL17 and not on the basis of radioactivity incorporated per unit weight of ligand. Thus, the experimentally determined value represents a true measure of the specific *binding* activity of the ligand, whereas the value supplied by the manufacturer gives the

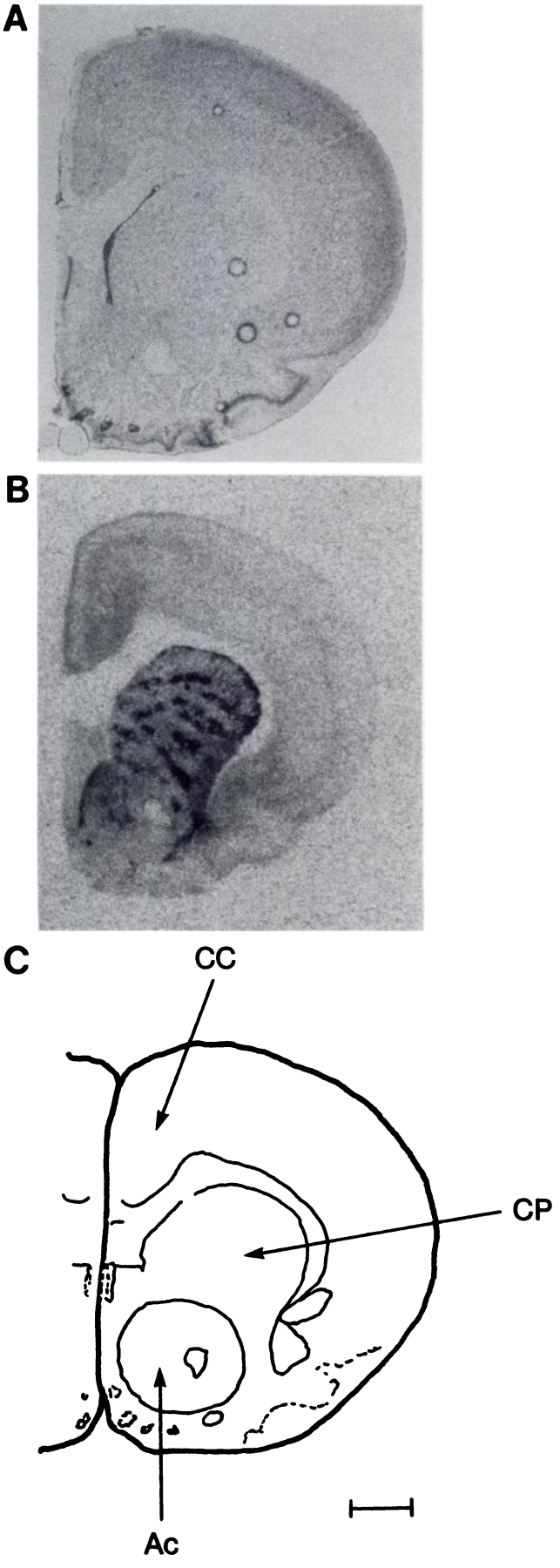

Fig. 6. Autoradiographic localization of [^{3}H]-PL17 showing typical μ-receptor "patches" in caudate-putamen. A. Nissl stain. B. Autoradiography. The photograph shows the observation of autoradiographic film under bright-field illumination. C. Schematic representation of cytoarchitecture of the section shown in A and B. *Ac*, accumbens nucleus; *CC*, cingulate cortex; *CP*, caudate-putamen nucleus. *Calibration bar* represents 1 mm.

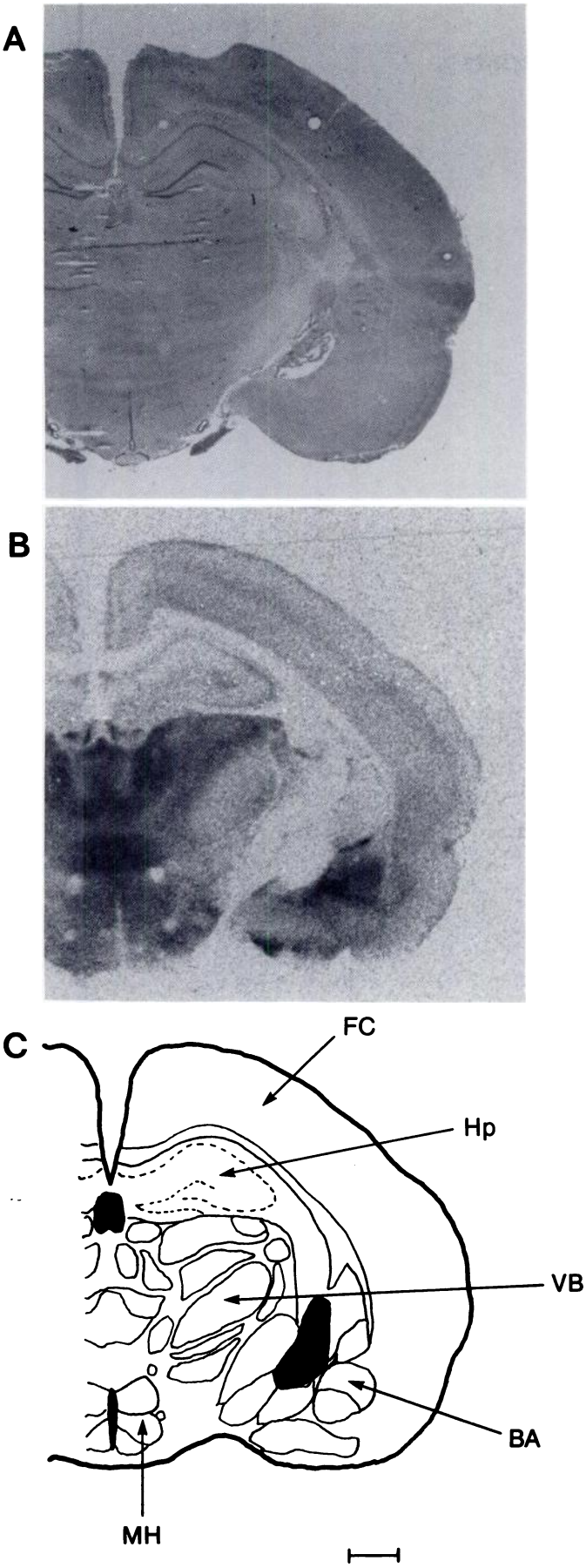

specific *radioactivity* of the ligand. These numbers are not necessarily identical. Furthermore, the presence of a single radioactive peak on chromatography of the radioligand (as in Fig. 1) does not guarantee that the radiolabeled ligand is pure. Comparison of the specific activity (determined by the method above) before and after the chromatography of Fig. 1 showed an ~2.5-fold increase after purification. Such errors in specific activity would in general affect the values for dissociation constants and site numbers but not the shape of displacement curves or Scatchard plots. The most obvious consequence would be a lack of agreement between values determined using different batches of ligand or in different laboratories. This analysis applies to equilibrium measurements; different binding kinetics of radiolabel versus impurities may further complicate the analysis. Other problems may arise; for instance, the K_d values derived from Scatchard plots are often used to calculate inhibition constants from IC_{50} values (Eq. 1). This compounds the errors since any impurities in the radiolabel may be different from those in the corresponding unlabeled ligand. Furthermore, complex curve-filling procedures require reasonably accurate initial estimates of various parameters to ensure convergence (28).

Saturation binding studies of [^{3}H]-PL17 binding to rat brain membranes gave a linear Scatchard plot (Fig. 4) with an apparent K_d of 6 nM in excellent agreement with previously published values (22). Although a linear Scatchard plot is consistent with binding to a single noninteracting site, more complicated models can also result in (apparently) linear Scatchard plots (19, 29). Furthermore, the experimental scatter at high bound/free (low bound) can make detection of nonlinearity difficult.

Both sodium ions and guanyl nucleotides decreased the binding of [^{3}H]-PL17 to rat brain membranes as observed for other opioid agonists. As shown in Fig. 4, this decrease seemed to be primarily due to a reduced number of binding sites. Although early studies (30–32) suggested that these agents decrease ligand affinity, more recent studies in the NG108-15 cell line (which contains only δ-receptors) have shown the effect to be more complex. Law *et al.* (33) reported that Na^+ caused a decrease in the number of high affinity [^{3}H]DADLE-binding sites with a corresponding appearance of sites of lower affinity. [^{3}H]-PL17 binding showed a similar decrease in the high affinity binding sites in the presence of Na^+; lower affinity sites were not detected. The inability to detect low affinity sites may be intrinsic to the μ-receptor type or an experimental difficulty (i.e., difficulty of obtaining accurate data at very high ligand and due to high nonspecific binding). As expected, the effects of Na^+ were potentiated by Gpp(NH)p; under these conditions the binding was so low that the mechanism of inhibition could not be determined. On pretreatment with guanyl nucleotides, however, there was an increase in binding sites when binding was measured in the presence of Mg^{2+} (see Results). Thus, the effects of guanyl nucleotides on [^{3}H]-PL17 depended on the nature of the cation (Na^+ or Mg^{2+}) present, in agreement with earlier studies using less selective ligands (23).

As with saturation binding analysis, displacement curves of [^{3}H]-PL17 by various opioid ligands could be described in terms of simple competitive inhibition at a single site (Fig. 5, Table

Fig. 7. Binding of [^{3}H]-PL17 to a coronal section from rat brain. Identification of panels is as in Fig. 6. *FC*, frontal cortex; *Hp*, hippocampus; *VB*, ventrobasal complex; *BA*, basal amygdala; *MH*, medial hypothalamus. The *calibration bar* in C represents 1 mm.

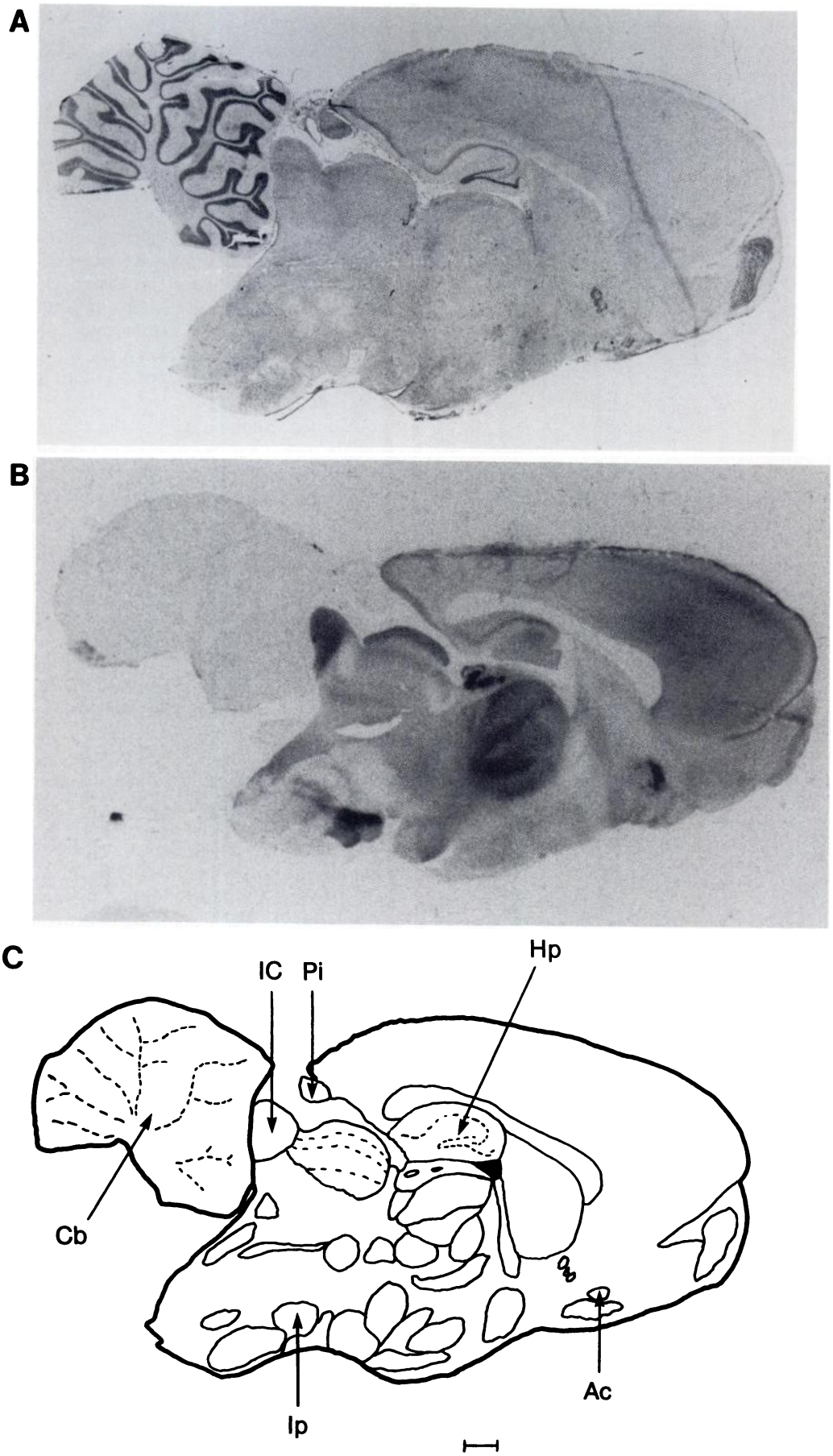

Fig. 8. [^{3}H]-PL17 labeling as evidenced in a sagittal section from rat brain. Identification of panels is as in Figs. 6 and 7. *Calibration bar* represents 1 mm. *Cb*, cerebellum; *IC*, inferior colliculus; *Pi*, pineal; *Hp*, hippocampus; *Ac*, accumbens nucleus; *Ip*, interpeduncular nucleus.

1). Although we cannot rule out the existence of multiple μ-receptor subtypes on the basis of the studies reported here with [^{3}H]-PL17, there was no suggestion of binding more complex than that expected for a single receptor site. More detailed studies will be needed in order to more fully understand the significance of the μ_1 sites. It should be noted that the previous studies reporting μ_1-type binding (17, 20) involved use of ligands with appreciable affinities for both μ- and δ-receptors, whereas we have been able to ignore the minute portion of [^{3}H]-PL17 binding to δ-receptors. In light of this difference and the different results, it would seem fruitful to reexamine previous results (17, 20) in terms of other models (e.g., allosteric models) which could account for the very high affinity sites in terms of induced rather than preexisting sites. Data suggesting such allosteric interactions for δ-sites in neuroblastoma sites have recently been presented (33, 34).

As expected, the localization of μ-receptors in rat brain by autoradiography with [^{3}H]-PL17 was very similar to that reported previously (7). [^{3}H]-PL17 has two distinct advantages over other ligands for such studies. First, there is the high selectivity for the μ-receptor type, and, second, the ligand exhibits very low nonspecific binding. (The second advantage may be a consequence of the first.) As such, [^{3}H]-PL17 should be very useful for quantitative autoradiography of μ-receptors.

Acknowledgments

We thank Mark A. Collins for expert technical assistance.

References

1. Gilbert, P. E., and W. R. Martin. The effects of morphine- and nalorphine-like drugs in the nondependent, morphine-dependent and cyclazocine-dependent chronic spinal dog. *J. Pharmacol. Exp. Ther.* **198**:66–82 (1976).
2. Martin, W. R., C. G. Eades, J. A. Thompson, R. E. Huppler, and P. E. Gilbert. The effects of morphine- and nalorphine-like drugs in the nondependent and morphine-dependent chronic spinal dog. *J. Pharmacol. Exp. Ther.* **197**:517–532 (1976).
3. Lord, J. H., A. A. Waterfield, J. Hughes, and H. W. Kosterlitz. Endogenous opioid peptides: multiple agonists and receptors. *Nature (Lond)* **267**:495–499 (1977).
4. Chang, K.-J., and P. Cuatrecasas. Multiple opiate receptors: enkephalins and morphine bind to receptors of different specificity. *J. Biol. Chem.* **254**:2610–2618 (1979).
5. Chang, K.-J., S. G. Blanchard, and P. Cuatrecasas. Benzomorphan sites are ligand recognition sites of putative ϵ-receptors. *Mol. Pharmacol.* **26**:484–488 (1984).
6. Young W. S. III, and M. J. Kuhar. A new method for receptor autoradiography: [^{3}H]opioid receptors in rat brain. *Brain Res.* **179**:255–270 (1979).
7. Goodman, R. R., S. H. Snyder, M. J. Kuhar, and W. S. Young III. Differentiation of delta and mu opiate receptor localizations by light microscopic autoradiography. *Proc. Natl. Acad. Sci. USA* **77**:6239–6243 (1980).
8. Herkenham, M., and C. B. Pert. *In vitro* autoradiography of opiate receptors in rat brain suggests loci of "opiatergic" pathways. *Proc. Natl. Acad. Sci. USA* **77**:5532–5536 (1980).
9. Valdes, F., B. Crain, K.-J. Chang, and J. McNamara. Radiohistochemical localization of opiate receptors in rat brain: the benzamorphan binding site. *Soc. Neurosci. Abstr.* **8**:647 (1982).
10. Bowen, W. D., S. Gentleman, M. Herkenham, and C. B. Pert. Interconverting μ and δ forms of the opiate receptor in rat striatal patches. *Proc. Natl. Acad. Sci. USA* **78**:4818–4822 (1981).
11. Rothman, R. B., and T. C. Westfall. Morphine allosterically modulates the binding of [^{3}H]leucine enkephalin to a particulate fraction of rat brain. *Mol. Pharmacol.* **21**:538–547 (1982).
12. Rothman, R. B., and T. C. Westfall. Allosteric coupling between morphine and enkephalin receptors *in vitro*. *Mol. Pharmacol.* **21**:548–577 (1982).
13. Pasternak, G. W., S. R. Childers, and S. H. Snyder. Opiate analgesia: evidence for mediation by a subpopulation of opiate receptors. *Science (Wash. D. C.)* **208**:514–516 (1980).
14. Pasternak, G. W. Multiple opiate receptors: [^{3}H]ethylketocyclazocine receptor binding and ketocyclazocine analgesia. *Proc. Natl. Acad. Sci. USA* **77**:3691–3694 (1980).
15. Zhang, A. Z., and G. W. Pasternak. Opiates and enkephalins: a common binding site mediates their analgesic actions in rats. *Life Sci.* **29**:843–851 (1981).
16. Hazum, E., K.-J. Chang, P. Cuatrecasas, and G. W. Pasternak. Naloxone irreversibly inhibits the high affinity binding of [^{125}I]D-Ala^2-D-Leu^5-enkephalin. *Life Sci.* **28**:2973–2979 (1981).
17. Wolozin, B. L., and G. W. Pasternak. Classification of multiple morphine and enkephalin binding sites in the central nervous system. *Proc. Natl. Acad. Sci. USA* **78**:6181–6185 (1981).
18. Pfeiffer, A., and A. Herz. Discrimination of three opiate receptor binding sites with the use of a computerized curve-fitting technique. *Mol. Pharmacol.* **21**:266–271 (1982).
19. Rothman, R. B., R. W. Barrett, and J. L. Vaught. Multidimensional analysis of ligand binding data: application to opioid receptors. *Neuropeptides* **3**:367–377 (1983).
20. Lutz, R. A., R. A. Cruciani, T. Costa, P. J. Munson, and D. Rodbard. A very high affinity opioid binding site in rat brain: demonstration by computer modeling. *Biochem. Biophys. Res. Commun.* **122**:265–269 (1984).
21. Chang, K.-J., A. Killian, E. Hazum, P. Cuatrecasas, and J.-K. Chang. Morphiceptin (NH_2-Tyr-Pro-Phe-Pro-$CONH_2$): a potent and specific agonist for morphine (μ) receptors. *Science (Wash. D. C.)* **212**:75–77 (1981).
22. Chang, K.-J., E. T. Wei, A. Killian, and J.-K. Chang. Potent morphiceptin analogs: structure activity relationships and morphine-like activities. *J. Pharmacol. Exp. Ther.* **227**:403–408 (1983).
23. Chang, K.-J., S. Blanchard, and P. Cuatrecasas. Unmasking of magnesium-dependent high-affinity binding sites for [D-Ala^2, D-Leu^5]enkephalin after pretreatment of brain membranes with guanine nucleotides. *Proc. Natl. Acad. Sci. USA* **80**:940–944 (1983).
24. Paxinos, G., and C. Watson. *The Rat Brain in Stereotoxic Coordinates.* Academic Press, New York (1982).
25. Cheng, Y.-C., and W. H. Prusoff. Relationship between the inhibition constant (K_i) and the concentration of inhibitor which causes 50 per cent inhibition (I_{50}) of an enzymatic reaction. *Biochem. Pharmacol.* **22**:3099–3108 (1973).
26. Blanchard, S. G., U. Quast, K. Reed, T. Lee, M. I. Schimerlik, R. Vandlen, T. Claudio, C. D. Strader, H.-P. Moore, and M. A. Raftery. Interaction of [^{125}I]-α-bungarotoxin with acetylcholine receptor from *Torpedo californica*. *Biochemistry* **18**:1875–1883 (1979).
27. Scatchard, G. The attractions of proteins for small molecules and ions. *Ann. N. Y. Acad. Sci.* **51**:660–672 (1949).
28. Munson, P. J., R. A. Cruciani, R. A. Lutz, and D. Rodbard. New methods for characterization of complex receptor systems involving three or more binding sites: application to brain opiate receptors. *J. Recept. Res.* **4**:339–355 (1984).
29. Quast, U., M. Schimerlik, and M. A. Raftery. Stopped flow kinetics of carbamylcholine binding to membrane bound acetylcholine receptor. *Biochem. Biophys. Res. Commun.* **81**:955–964 (1978).
30. Pert, C. B., and S. H. Snyder. Opiate receptor binding of agonists and antagonists affected differentially by sodium. *Mol. Pharmacol.* **10**:868–879 (1974).
31. Simon, E. J., and J. Groth. Kinetics of opiate receptor inactivation by sulfhydryl reagents: evidence for a conformational change in the presence of sodium ions. *Proc. Natl. Acad. Sci. USA* **72**:2404–2407 (1975).
32. Blume, A. J. Interaction of ligands with the opiate receptors of brain membranes: regulation by ions and nucleotides. *Proc. Natl. Acad. Sci. USA* **75**:1713–1717 (1978).
33. Law, P.-Y., D. S. Hom, and H. H. Loh. Multiple affinity states of opiate receptor in neuroblastoma × glioma NG108-15 hybrid cells: opiate agonist association rate is a function of receptor occupancy. *J. Biol. Chem.* **260**:3561–3569 (1985).
34. Costa, T., M. Wüster, C. Gramsch, and A. Herz. Multiple states of opioid receptors may modulate adenylate cyclase in intact neuroblastoma × glioma hybrid cells. *Mol. Pharmacol.* **28**:146–154 (1985).
35. Chang, K.-J., P. Cuatrecasas, E. T. Wei, and J.-K. Chang. Analgesic activity of intracerebroventricular administration of morphiceptin and β-casomorphins: correlation with the morphine (μ) receptor binding affinity. *Life Sci.* **30**:1547–1551 (1982).

Send reprint requests to: Dr. K.-J. Chang, Department of Molecular Biology, Burroughs Wellcome Co., Research Triangle Park, NC 27709.